

ON THE USE OF DIMENSION AND LACUNARITY FOR COMPARING THE RESONANT BEHAVIOR OF CONVOLUTED WIRE ANTENNAS

M. Comisso

Dipartimento di Elettrotecnica, Elettronica ed Informatica
University of Trieste
Via A. Valerio 10, Trieste 34127, Italy

Abstract—This paper analyzes the possibility to use dimension and lacunarity for comparing the resonant behavior of different convoluted wire antennas, including prefractal dipoles. Since previous studies have proved that the Hausdorff fractal dimension is not suitable for antenna comparison purposes, this work proposes the adoption of a different approach for evaluating the dimension by using the measurement at scale δ , which is more suitable for analyzing real phenomena. The results provided by this measure are compared to those obtained by using the average lacunarity. The objective is to verify if, given two convoluted wire dipoles, the dimension and average lacunarity provide sufficient information to infer which dipole exhibits the lower resonances.[†]

1. INTRODUCTION

The study and design of small antennas able to provide multiple resonant frequencies represents one of the fundamental topics of current research efforts in antenna development. The geometrical characteristics have a strong impact on the resonances of a radiator, since a proper selection of the geometry can enable the reduction of the overall antenna size simultaneously, guaranteeing a multi-band behavior. Accordingly, several research papers have proposed novel antenna design techniques based on meander line curves and fractal geometry [1–9]. In many cases, the selection of the geometry satisfying the design specifications requires accurate electromagnetic simulations

Corresponding author: M. Comisso (mcomisso@units.it).

[†] A preliminary, partial version of this paper has been presented at the 2009 APS/URSI International Symposium, Charleston, South Carolina (USA), 1–5 Jun. 2009.

and the adoption of proper optimization techniques. In fact, usually the theoretical prediction of the resonant behavior of an antenna is a problem difficult to solve, even if some efforts have been made to better characterize the relationship between the antenna geometry and electromagnetic characteristics of the radiator [10–16]. In particular, in fractal antenna design, recent studies have investigated the possibility to relate the Hausdorff fractal dimension to the position of the resonant frequencies of a convoluted dipole [10, 11]. However, as shown in [12], the Hausdorff dimension alone, which may be significant only for prefractal antennas, does not play a decisive role in determining the resonant behavior of prefractal dipoles. Besides, several studies confirm that many convoluted (non-prefractal) radiators can provide multiple resonances and/or miniaturization capabilities [13]. Hence, the fractal dimension, as it is defined in fractal analysis [17], seems not suitable to characterize the real curves that are adopted in antenna design. Recently, another mathematical quantity, called lacunarity, has been adopted to examine the resonant behavior of some prefractal wire antennas, such as the Von Koch and Minkowski dipoles [14, 15]. With respect to Hausdorff dimension, lacunarity can be applied both to prefractal and non-prefractal antennas. However, the possibility to compare the resonant behavior of two wire antennas moving from the knowledge of their geometrical characteristics remains an open issue.

This paper investigates the possibility to use dimension and average lacunarity for comparing the resonant frequencies of convoluted wire antennas, including prefractal and meander line dipoles. A different method for calculating the dimension is proposed. This method is based on the measurement at scale δ , which is often adopted to numerically analyze real phenomena. The results provided by this measure are combined to those obtained by using the average lacunarity in order to study which characteristics of the resonances can be inferred from these two mathematical quantities. The purpose is to verify if, given two convoluted wire dipoles having the same height and the same total length, the dimension and average lacunarity provide sufficient information to infer which dipole exhibits the lower resonances.

The paper is organized as follows. Section 2 introduces the geometries considered in the comparison. Section 3 describes the adopted mathematical quantities. Section 4 presents and discusses the main results. Section 5 summarizes the paper contributions and the most important conclusions.

2. GEOMETRY DESCRIPTION

The dipoles considered in the comparison have the same height $H = 1$ m, the same wire diameter $a = 1.5$ mm and are generated according to three geometries: Minkowski geometry, generalized Von Koch geometry, and rectangular meander line (Fig. 1). The radiators generated using the first two geometries are prefractal antennas, while non-prefractal dipoles are obtained employing the latter geometry. In Fig. 1 the symbol n denotes the iteration, when referred to the prefractals, while it denotes the number of turns, when referred to the meander line.

The generation procedure of the Minkowski curve moves from a line segment of height $H/2$, called *initiator* and corresponding to the iteration $n = 0$, and from the line obtained at the first iteration, called *generator* (Fig. 1(a)). The generator is composed by three vertical segments, having a length equal to one-third of the original height, and two horizontal segments, having a length equal to $w/3$ of the original height, where the parameter w ($0 \leq w \leq 1$) is called *indentation*. The Minkowski prefractal at n -th iteration is obtained replacing by the generator each straight segment of the prefractal corresponding to the $(n - 1)$ -th iteration, thus obtaining a curve having a length:

$$L = \frac{H}{2} \left(1 + \frac{2}{3}w \right)^n. \quad (1)$$

By iterating this process for n approaching infinity one obtains the Minkowski curve, whose Hausdorff dimension D_H can be obtained by numerically solving the following equation [1]:

$$3 + 2w^{D_H} - 3^{D_H} = 0. \quad (2)$$

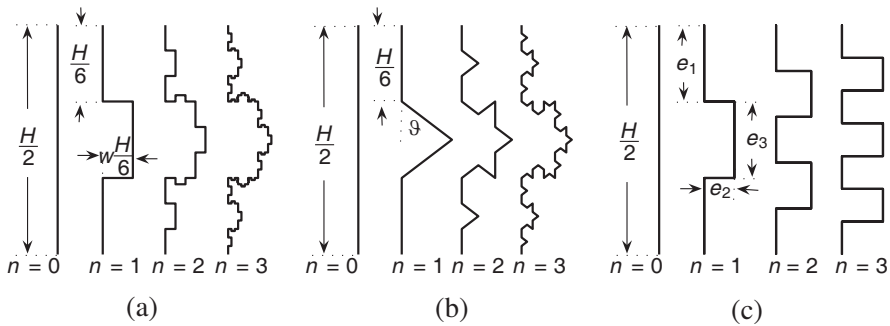


Figure 1. Adopted geometries: (a) Minkowski geometry, (b) Von Koch geometry, (c) rectangular meander line geometry.

Observe that, when n approaches infinity, the Minkowski curve remains confined in a finite area, but its length approaches infinity.

An identical procedure, but using a different generator, leads to the generalized Von Koch prefractal (Fig. 1(b)). In this case the generator is composed by four segments of length $H/[4(1 + \cos \theta)]$, where θ ($0 \leq \theta < \pi/2$) represents the *indentation angle*. The successive iterations of the curve are obtained replacing each straight segment by the generator. This procedure leads to a curve having a length:

$$L = \frac{H}{2} \left(\frac{2}{1 + \cos \theta} \right)^n, \quad (3)$$

at the n -th iteration and a Hausdorff dimension for n approaching infinity that can be evaluated as [14]:

$$D_H = \frac{\ln 4}{\ln[2(1 + \cos \theta)]}. \quad (4)$$

Finally, the rectangular meander line in Fig. 1(c) is generated according to the classical Euclidean geometry, and hence it does not belong to the set of prefractal antennas. In this case the symbol n denotes the number of turns, and the size of each wire segment is selected according to the desired total length. More precisely, the pitch is selected as $e_1 = e_3 = H/[2(2n + 1)]$ and the width as $e_2 = (2L - H)/(4n)$.

The simulation tool adopted for evaluating the resonances of the center-fed dipoles generated according to the three geometries is the Numerical Electromagnetic Code (NEC-2) [18], while the geometrical structures are developed by recursive loops in Matlab and then passed to the electromagnetic simulator. The dipoles are discretized by using a minimum wire segment ε that satisfies the relationships $10^{-3}\lambda \leq \varepsilon \leq 10^{-1}\lambda$, where λ is the wavelength, and $\varepsilon/(a/2) \geq 2$. These practical rules satisfy the convergence requirements of NEC2 and guarantee the accuracy of the calculated resonances.

3. DIMENSION AND LACUNARITY

Several definitions of fractal dimension have been formulated in fractal analysis. The most diffused and important one is the definition provided by Hausdorff, which can be applied to any fractal set. A complete mathematical treatment of this quantity can be found in [17]. Unfortunately, Hausdorff dimension is unable to provide sufficient information to compare prefractal dipoles developed considering different generation rules [12]. This limitation may be mainly due to the fact that the Hausdorff dimension characterizes a fractal (ideal) curve that, as a matter of fact, is rather different from the geometries

adopted in practical applications, where only dipoles corresponding to low iteration values are realizable. In fact, the Hausdorff dimension is independent of the fractal iteration and total length of the curve that determines the geometry of a dipole. Instead, for antenna research purposes, a measure of dimension more adherent to the actual geometry of a dipole may be desirable. For this aim, in this study we propose the use of the *measurement at scale δ* [17], whose computation can be performed as follows.

Consider a set Ω that represents a binary image consisting of a plane curve in the two-dimensional space. The set Ω can be digitized in an underline binary matrix in which the zero entry (black) represents an empty pixel, and the one entry (white) denotes the presence of a full pixel (belonging to the plane curve). Consider now a regular grid composed by square boxes of edge δ and evaluate the number of boxes containing at least one full pixel $N(\delta)$ (Fig. 2). The measurement at scale δ , which will be indicated in the following using the symbol D , can be obtained by calculating $N(\delta)$ for several scales δ , chosen between a minimum value δ_{\min} and maximum one δ_{\max} with a step δ_s . If the

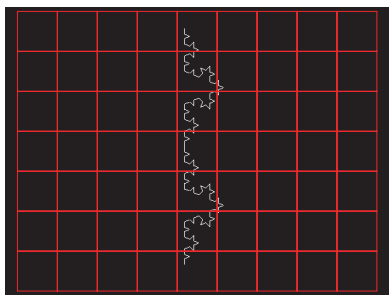


Figure 2. Example of a binary image having a resolution of 432×576 pixels and representing a Von Koch dipole at the third iteration with an example of grid (in red) generated using a box of $\delta = 60$ pixels. Observe that, since each square box of the grid has 60 pixels, we obtain a 7×9 grid.

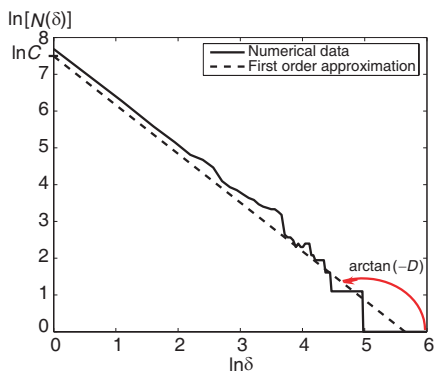


Figure 3. Numerical evaluation and first order approximation of $\ln[N(\delta)]$ as a function of $\ln\delta$ for the image in Fig. 2. The opposite of the slope of the straight line provides the dimension.

function $N(\delta)$ obeys a power law:

$$N(\delta) \cong C\delta^{-D}, \quad (5)$$

where C is a constant, (5) can be reformulated in a log-log scale as:

$$\ln[N(\delta)] \cong \ln C - D \ln \delta. \quad (6)$$

In general, for real digitized curves, $N(\delta)$ does not exactly obey a power law, hence, a first-order approximation of $\ln[N(\delta)]$ as a function of $\ln \delta$ is required. The slope of this approximating straight line is equal to $-D$ (Fig. 3). For ideal fractals D must be evaluated by considering the limit of $-\ln[N(\delta)]/\ln \delta$ for δ approaching zero, while for real curves a finite range of δ can be used. The adoption of the measurement at scale δ as a dimension for characterizing the set Ω enables to account for the actual shape of a curve. Even if, in a strict mathematical sense, D may be not considered a dimension, this quantity is appealing for computational and experimental purposes, when real phenomena must be analyzed [19]. Observe that, differently from the Hausdorff dimension, the measurement at scale δ can also be applied to non-prefractal curves and hence allows to analyze the entire family of convoluted wire dipoles.

Another quantity adopted to characterize a fractal set is the lacunarity, which provides information regarding the heterogeneity of an object and can be viewed as a measure of the distribution of the gaps in its topology [20]. More precisely, lacunarity is able to quantify the deviation from the translational invariance of the considered object by describing the distribution of gaps within a set at multiple scales. Thus, when an object becomes more lacunar, the spatial arrangement of the gaps in its geometrical structure becomes more heterogeneous. Similar to the measurement at scale δ , lacunarity can be evaluated both for fractal and non-fractal sets and hence is suitable for investigating both prefractal and non-prefractal curves.

For the above defined binary set Ω , the lacunarity can be evaluated considering the mass distribution probability of pixels $P(q, \delta)$, which can be obtained from the statistic of the boxes at scale δ containing q ($1 \leq q \leq q_{\max}$) full pixels. The lacunarity of Ω at scale δ is defined as the ratio between the second moment of $P(q, \delta)$ and the square of its mean [21]:

$$\Lambda(\delta) = \frac{\sum_{q=1}^{q_{\max}} q^2 P(q, \delta)}{\left[\sum_{q=1}^{q_{\max}} q P(q, \delta) \right]^2}. \quad (7)$$

A numerical method for the estimation of $\Lambda(\delta)$ is the gliding-box algorithm [21]. This algorithm scans the binary matrix that digitizes the considered set Ω using square boxes of different sizes, starting from the minimum one δ_{\min} and increasing the size by a step δ_s until the maximum box size δ_{\max} is reached. For each box size the scan begins from the upper left corner of the matrix. Then, the box is horizontally moved by a certain number of columns ρ and, once the left end of the matrix is reached, the box is vertically moved by ρ lines. For each position the number of full pixels is evaluated, and so the number of boxes of side δ and mass q , $M(q, \delta)$, can be obtained. The mass distribution probability of pixels $P(q, \delta)$ is the ratio between $M(q, \delta)$ and the number of boxes at scale δ . Once $P(q, \delta)$ has been estimated, the lacunarity can be calculated using (7). Since $\Lambda(\delta)$ is dependent on the box size, an average measure is proposed in [14]. In this study, this measure is reformulated according to the adopted discretized approach, thus defining the average lacunarity as:

$$\bar{\Lambda} = \ln \frac{\delta_s \cdot \sum_{\delta=\delta_{\min}}^{\delta_{\max}} \Lambda(\delta)}{\delta_{\max} - \delta_{\min}}. \quad (8)$$

Both adopted measures, D and $\bar{\Lambda}$, are influenced by the minimum box size δ_{\min} , the maximum one δ_{\max} , and the box size step δ_s . Besides, the lacunarity depends also on the shift ρ . Since we are comparing dipoles having the same height, length and wire radius, we expect that the resonances provided by the electromagnetic simulator, even if often distinguishable, are rather close. Hence, if we want to investigate the possible information that can be obtained from the dimension and average lacunarity in terms of resonant frequencies, a really accurate computation of D and $\bar{\Lambda}$ must be performed. Thus, many dense grids must be used. Accordingly, remembering that each image describing a dipole is digitized in a 432×576 binary matrix (Fig. 2), the parameters are selected as $\delta_{\min} = 1$, $\delta_{\max} = 431$, $\delta_s = 1$, and $\rho = 1$. These choices lead to a considerable increase of the computation time for the gliding-box algorithm, but guarantee a really accurate estimation because all possible grids are taken into account. Once the parameter setting is completed, a further element must be carefully taken into account to have a good correspondence between the physical dipoles simulated by NEC2 and the images analyzed in terms of dimension and lacunarity. This element is the wire radius, which determines the width of the curve in the image. Consider first that, as described in Section 2, we have a cylindrical wire having a diameter equal to 1.5 mm, corresponding to an equivalent strip of width equal to $2 \cdot 1.5 = 3$ mm [22]. Besides, observe that the dipole of height equal to

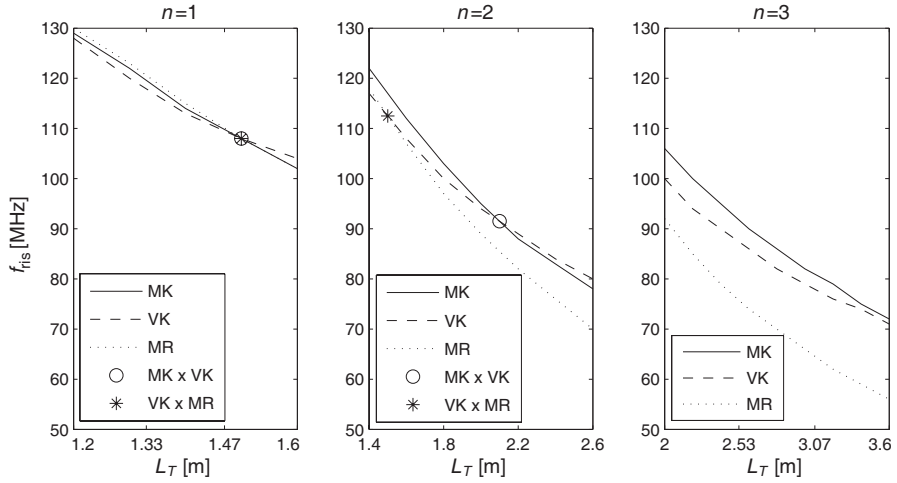


Figure 4. First resonant frequency of the three considered dipoles as a function of the total length for different values of n : MK — Minkowski, VK — Von Koch, MR — meander line.

one meter is plotted with a height of 354 pixels in a 432×576 binary image (Fig. 2). Therefore, we can obtain the correctly rescaled width (in pixels) of the curve in the image as $3 \cdot 354/1000 \cong 1$. Hence, the equivalent width in the processed image is equal to one pixel.

4. NUMERICAL RESULTS

This section presents the resonances provided by NEC2 simulations and discusses the results obtained in terms of dimension and average lacunarity. Both the gliding-box algorithm and measurement at scale δ are implemented in Matlab. Figs. 4–6 show the first three resonant frequencies of the considered dipoles as a function of the total length $L_T = 2L$, while Figs. 7–9 report, still as a function of L_T , the Hausdorff dimension, the measurement at scale δ , and the average lacunarity, respectively. The markers in the figures have been inserted to emphasize the possible interceptions between the curves in order to simplify the interpretation of the results.

We can immediately observe from a comparison between Figs. 4–6 and Fig. 7 that, as already proved in [12], the Hausdorff dimension does not provide significant information regarding the relative differences between the resonances of dipoles generated according to different geometrical rules. In fact, from the point of view of D_H , the Von

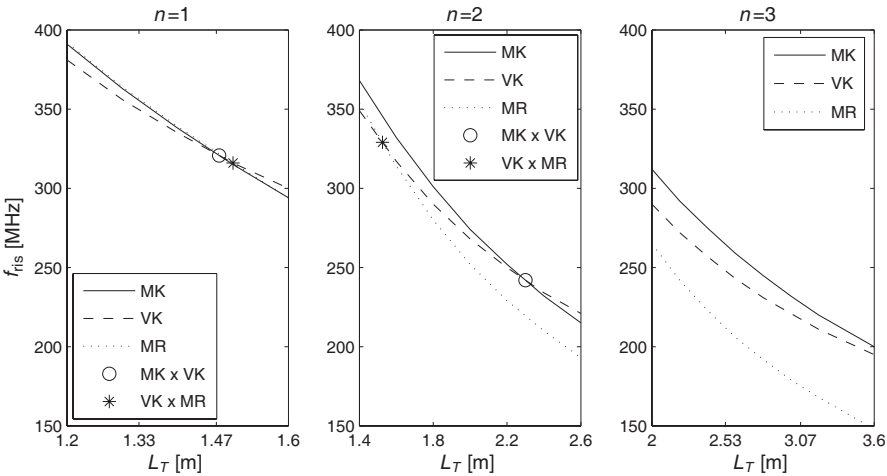


Figure 5. Second resonant frequency of the three considered dipoles as a function of the total length for different values of n : MK — Minkowski, VK — Von Koch, MR — meander line.

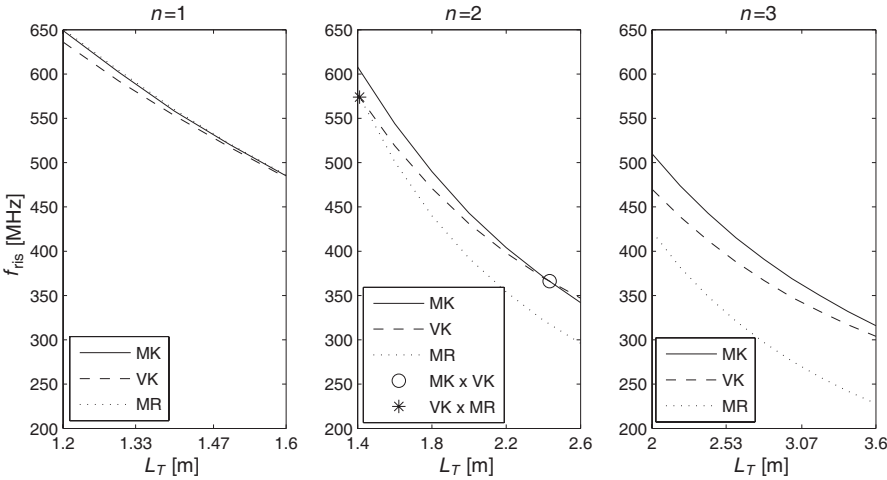


Figure 6. Third resonant frequency of the three considered dipoles as a function of the total length for different values of n : MK — Minkowski, VK — Von Koch, MR — meander line.

Koch geometry should be able to always provide lower resonances than the Minkowski one for $n = 2, 3$, while the opposite should happen for $n = 1$, but this behavior is not confirmed by the resonance curves.

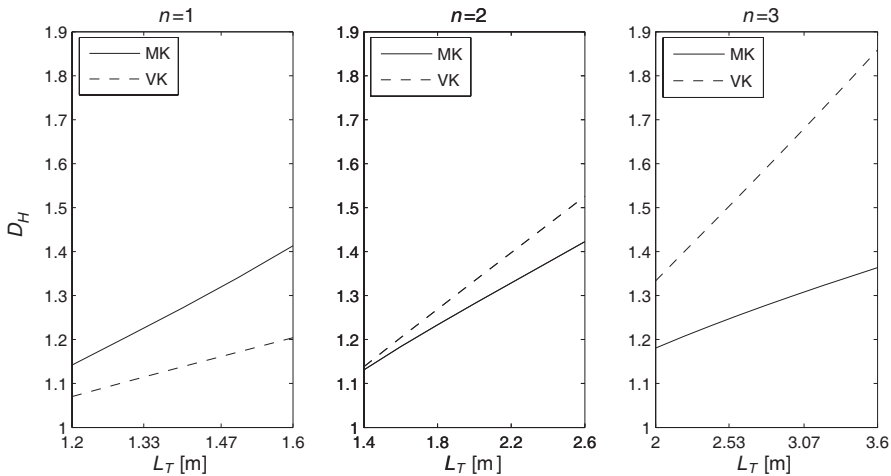


Figure 7. Hausdorff dimension of the two considered prefractal dipoles as a function of the total length for different values of n : MK — Minkowski, VK — Von Koch.

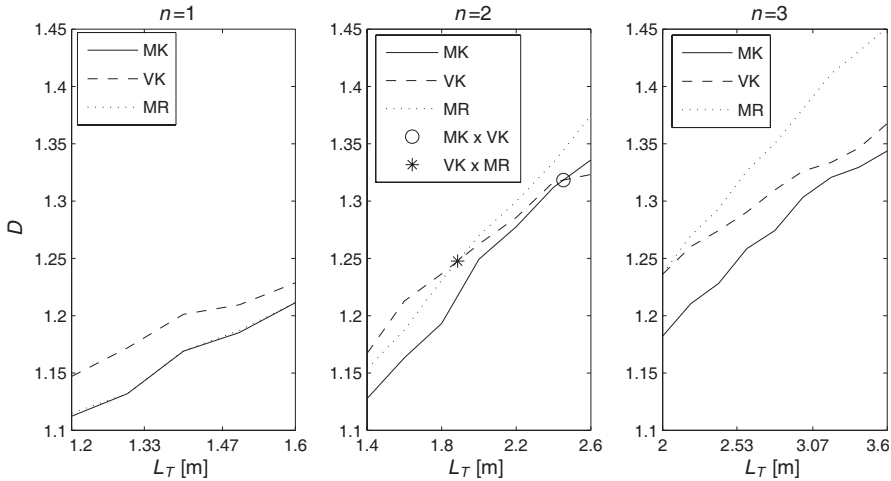


Figure 8. Measurement at scale δ of the three considered dipoles as a function of the total length for different values of n : MK — Minkowski, VK — Von Koch, MR — meander line.

Besides, D_H cannot be evaluated for the rectangular meander line and hence is not general enough to describe all possible real convoluted dipoles. Observe that the possibility of having different values of D_H

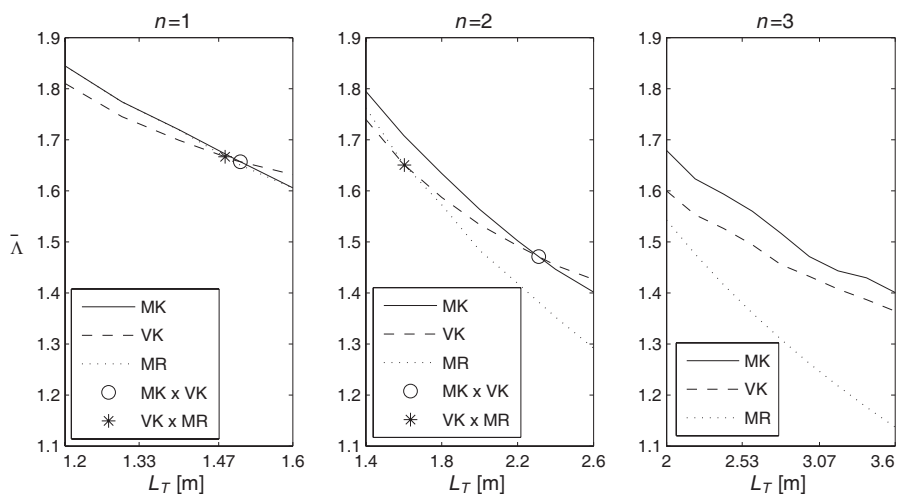


Figure 9. Average lacunarity of the three considered dipoles as a function of the total length for different values of n : MK — Minkowski, VK — Von Koch, MR — meander line.

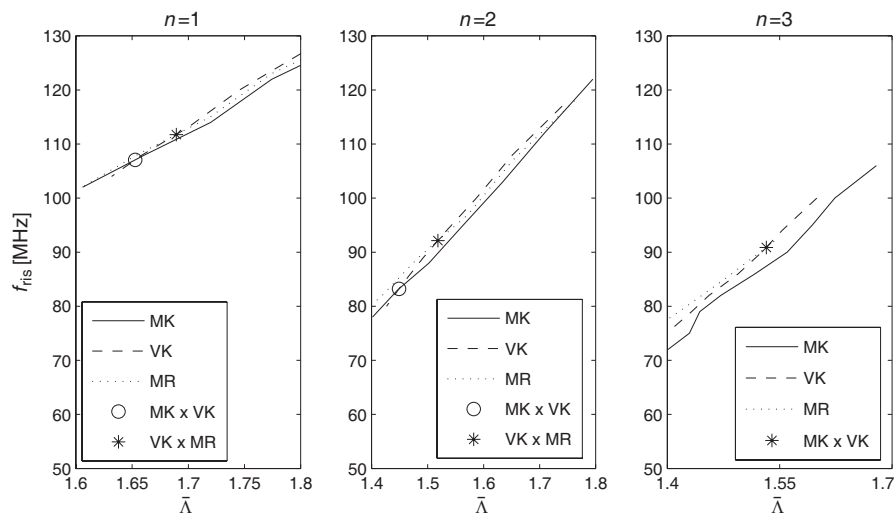


Figure 10. First resonant frequency of the three considered dipoles as a function of the average lacunarity for different values of n : MK — Minkowski, VK — Von Koch, MR — meander line.

for equal values of L_T and different values of n does not contradict the theory, which states that D_H is independent of the iteration. To this purpose, consider the following arguments, which are referred to the Minkowski curve but hold also for the Von Koch one. To obtain the same value of $L_T = 2L$ for two different values of n , we have to use two different values of the indentation w by inverting (1), thus obtaining two different values of D_H by solving (2). Therefore, to generate dipoles with the same L_T and different n , we have to refer to different fractal curves.

More information regarding the behavior of the resonances can be inferred from the measurement at scale δ (Fig. 8). It is worth to notice that, as expected, D is an increasing function of L_T , while the resonances are decreasing functions of L_T . This fact can be explained remembering that the dimension measures the space filling capabilities of an object. Therefore, we may expect a sort of reciprocity between the curves representing the resonances and those representing D . For example, comparing Figs. 4–6 to Fig. 8 for $n = 3$, we can observe that the higher is the dimension of a geometry, the lower are its resonances. In addition to the absence of interceptions for $n = 3$, the measurement at scale δ confirms the two interceptions for $n = 2$. Besides, D can also be applied to the rectangular meander line, enabling the comparison of this structure with the prefractal ones. Thus, the measurement at scale δ seems a more interesting quantity for comparison purposes with respect to Hausdorff dimension. The ability of D to provide a measure that is more adherent to the actual geometry of a dipole, as compared to D_H , may be explained remembering that the calculation of the measurement at scale δ is based on a sequence of grids at different scales that enables a more detailed analysis of the real shape of a dipole. However, D is still unable to describe the relative differences between the resonances for $n = 1$, and the positions of the interceptions for $n = 2$ are rather different from those shown in Figs. 4–6.

A considerable analogy can be noticed between Figs. 4–6 and the average lacunarity reported in Fig. 9. Observe that the lacunarity is related to the gaps present in a geometry, thus $\bar{\Lambda}$ is a decreasing function of L_T . The average lacunarity seems to provide an accurate information, since $\bar{\Lambda}$ has two interceptions for $n = 1$, two interceptions for $n = 2$ and no interceptions for $n = 3$. Besides, with respect to the curves describing D , the positions of the interceptions are closer to those of the resonance curves. This behavior can be explained observing that the lacunarity, being evaluated using the gliding-box algorithm, does not consider only boxes at different scales, as already done by the measurement at scale δ , but also considers the translation of these boxes, thus capturing the characteristics related to

the inhomogeneity of the geometrical structure of a dipole.

Even if the above results are encouraging, we can observe in Figs. 4–6 that the three sets of curves describing the resonances show a similar relative behavior for a given n value, but the relative positions of these curves are not identical. In particular, for a given n , the interceptions do not necessarily appear for all orders of resonance and, when the interceptions are present for all orders of resonance, they do not correspond to an identical L_T value. On the other hand, for given values of n and L_T , the measurement at scale δ and the average lacunarity currently provide a unique information that cannot hold, in general, simultaneously for all the three resonances. To emphasize the inability of $\bar{\Lambda}$ to completely characterize the resonances, Fig. 10 reports the first resonance as a function of the average lacunarity and confirms that two different dipoles with the same value of $\bar{\Lambda}$ can have different resonances. Even if the measurement at scale δ and the average lacunarity are unable, when taken individually, to completely characterize the resonant behavior of a convoluted dipole, we may not exclude the existence of a function dependent on the order of resonance and involving D and $\bar{\Lambda}$ together. To investigate this possibility we have carried out a further simulation by generating, for $n = 3$, a generalized Von Koch dipole with $\vartheta \cong 67.25^\circ$ and a Minkowski dipole with $w \cong 0.76$. These values are selected because they provide two different prefractal dipoles having the same value of measurement at scale δ ($D \cong 1.33$) and the same average lacunarity ($\bar{\Lambda} \cong 1.43$). In this case the three resonances of the Von Koch dipole occur at 79 MHz, 221 MHz, and 348 MHz, while those of the Minkowski dipole occur at 75 MHz, 210 MHz, and 332 MHz. Hence, equal values of D and $\bar{\Lambda}$ lead anyway to different resonances. This means that also average lacunarity and measurement at scale δ together are not sufficient to completely characterize the resonant behavior of a prefractal dipole.

It is worth to notice that, for the particular case of the Von Koch geometry, an empirical formula that relates the first resonant frequency to the Hausdorff dimension has been derived in [11], while another one relating the first resonant frequency to the average lacunarity has been presented in [14]. Furthermore, in [15], an analytical model that provides the resonant frequencies of the Minkowski dipole as a function of D_H has been described. Therefore, the proof provided in this study states the impossibility of characterizing the resonant behavior of a convoluted antenna in general by using only D_H , D and $\bar{\Lambda}$, but does not deny the existence of a relationship between the resonances and the considered mathematical quantities in some specific cases.

5. DISCUSSION AND CONCLUSIONS

The possibility to use dimension and average lacunarity for comparing the resonant behavior of different convoluted wire antennas has been investigated. Since previous studies have shown that the Hausdorff dimension does not play a decisive role in determining the resonances, the adoption of the measurement at scale δ has been proposed. The results have revealed that more information regarding the behavior of the resonances can be inferred from this measure with respect to the Hausdorff dimension, since the measurement at scale δ is evaluated adopting a numerical approach, that provides results more adherent to the actual geometry of a dipole. A better analogy has been observed between the average lacunarity and the resonances, thanks to the ability of the gliding-box algorithm to account for all possible translations of the boxes at different scales. A common advantage of the measurement at scale δ and the average lacunarity is their ability to analyze real curves, including both prefractal and non-prefractal dipoles. It is worth to notice, however, that even if the average lacunarity provides more accurate information with respect to the measurement at scale δ , this information is obtained at the cost of a considerable increase of the computation time because, to evaluate the lacunarity, all possible translations must be considered for each grid. Thus, differently from the Hausdorff dimension, the measurement at scale δ may be used for practical purposes, in order to perform a rough and fast comparison between two geometries. If the objective is the design of a convoluted dipole, the estimation of the measurement at scale δ may represent a first step to compare different possibilities before the accurate electromagnetic simulation. This possibility is partly allowed by the average lacunarity, which is a more accurate measure, but requires much more time for computation.

It is also worth to notice that the presented analysis has been performed considering dipoles with really similar characteristics (equal height, equal length, and equal wire radius), and hence with really similar resonances. Thus, the inability to completely characterize the resonant behavior of a convoluted dipole using the measurement at scale δ and the average lacunarity together, has been proved in extreme conditions. Therefore, this investigation excludes the complete control of these two quantities on the resonant behavior of a convoluted dipole, but does not exclude the possible existence of a direct relationship for some specific cases and, moreover, cannot exclude the possibility that the measurement at scale δ and the average lacunarity have a partial, perhaps strong, influence on the resonances.

ACKNOWLEDGMENT

This work is partly supported by the Italian Ministry of University and Research (MIUR) within the project SESAME (Scalable Efficient Secure Autonomic MESH networks).

REFERENCES

1. Gianvittorio, J. P. and Y. Rahmat-Samii, "Fractal antennas: A novel antenna miniaturization technique, and applications," *IEEE Antennas and Propagation Magazine*, Vol. 44, No. 1, 20–36, 2002.
2. Naghshvarian-Jahromi, M. and N. Komjani, "Novel fractal monopole wideband antenna," *Journal of Electromagnetic Waves and Applications*, Vol. 22, No. 2–3, 195–205, 2008.
3. Cui, G., Y. Liu, and S. Gong, "A novel fractal patch antenna with low RCS," *Journal of Electromagnetic Waves and Applications*, Vol. 21, No. 15, 2403–2411, 2007.
4. Chen, X. and K. Huang, "Wideband properties of fractal bowtie dipoles," *Journal of Electromagnetic Waves and Applications*, Vol. 20, No. 11, 1511–1518, 2006.
5. Ataeiseresht, R., C. H. Ghobadi, and J. Nourinia, "A novel analysis of minkowski fractal microstrip patch antenna," *Journal of Electromagnetic Waves and Applications*, Vol. 20, No. 8, 1115–1127, 2006.
6. Wu, W. and Y. H. Bi, "Switched-beam planar fractal antenna," *Journal of Electromagnetic Waves and Applications*, Vol. 20, No. 3, 409–415, 2006.
7. Yeo, U. B., J. N. Lee, J. K. Park, H. S. Lee, and H. S. Kim, "An ultra-wideband antenna design using sierpinski sieve fractal," *Journal of Electromagnetic Waves and Applications*, Vol. 22, No. 11–12, 1713–1723, 2008.
8. Salmasi, M. P., F. H. Kashani, and M. N. Azarmanesh, "A novel broadband fractal sierpinski shaped microstrip antenna," *Progress In Electromagnetics Research C*, Vol. 4, 179–190, 2008.
9. Khan, S. N., J. Hu, J. Xiong, and S. He, "Circular fractal monopole antenna for low VSWR UWB applications," *Progress In Electromagnetics Research Letters*, Vol. 1, 19–25, 2008.
10. Vinoy, K. J., J. K. Abraham, and V. K. Varadan, "Fractal dimension and frequency response of fractal shaped antennas," *IEEE Antennas and Propagation Society International Symposium*, Vol. 4, 222–225, Jun. 22–27, 2003.
11. Vinoy, K. J., J. K. Abraham, and V. K. Varadan, "On the

- relationship between fractal dimension and the performance of multi-resonant dipole antennas using Koch curves,” *IEEE Transactions on Antennas and Propagation*, Vol. 51, No. 9, 2296–2303, 2003.
12. González, J. M. and J. Romeu, “Experiences on monopoles with the same fractal dimension and different topology,” *IEEE Antennas and Propagation Society International Symposium*, Vol. 4, 218–221, Jun. 22–27, 2003.
 13. Best, S. R., “A discussion on the significance of geometry in determining the resonant behavior of fractal and other non-euclidean wire antennas,” *IEEE Antennas and Propagation Magazine*, Vol. 45, No. 3, 9–27, 2003.
 14. Sengupta, K. and K. J. Vinoy, “A new measure of lacunarity for generalized fractals and its impact in the electromagnetic behavior of Koch dipole antennas,” *Fractals*, Vol. 14, No. 4, 271–282, 2006.
 15. Comisso, M., “Theoretical and numerical analysis of the resonant behavior of the minkowski fractal dipole antenna,” *IET Microwaves, Antennas and Propagation*, Vol. 3, No. 3, 456–464, 2009.
 16. Ansarizadeh, M., A. Ghorbani, and R. A. Abd-Alhameed, “An approach to equivalent circuit modeling of rectangular microstrip antennas,” *Progress In Electromagnetics Research B*, Vol. 8, 77–86, 2008.
 17. Falconer, K., *Fractal Geometry: Mathematical Foundations and Applications*, John Wiley and Sons, New York, 1990.
 18. Burke, G. J. and A. J. Poggio, *Numerical Electromagnetic Code (NEC) Method of Moments*, Naval Ocean Systems Center, San Diego, CA, 1980.
 19. Martorella, M., F. Berizzi, and E. D. Mese, “On the fractal dimension of sea surface backscattered signal at low grazing angle,” *IEEE Transactions on Antennas and Propagation*, Vol. 52, No. 5, 1193–1204, 2004.
 20. Mandelbrot, B. B., *The Fractal Geometry of Nature*, W. H. Freeman and Company, New York, 1977.
 21. Allain, C. and M. Cloitre, “Characterizing the lacunarity of random and deterministic fractal sets,” *Physical Review A*, Vol. 44, No. 6, 3352–3558, 1991.
 22. Balanis, C. A., *Antenna Theory: Analysis and Design*, John Wiley and Sons, New York, 1997.